Development 137, 3405-3409 (2010) doi:10.1242/dev.052340
© 2010. Published by The Company of Biologists Ltd

Quantitative analyses link modulation of sonic hedgehog signaling to continuous variation in facial growth and shape

Nathan M. Young[1,*], H. Jonathan Chong[2,*], Diane Hu[1], Benedikt Hallgrímsson[3] and Ralph S. Marcucio[1,†]

SUMMARY

Variation is an intrinsic feature of biological systems, yet developmental biology does not frequently address population-level phenomena. Sonic hedgehog (SHH) signaling activity in the vertebrate forebrain and face is thought to contribute to continuous variation in the morphology of the upper jaw, but despite its potential explanatory power, this idea has never been quantitatively assessed. Here, we test this hypothesis with an experimental design that is explicitly focused on the generation and measurement of variation in multivariate shape, tissue growth, cellular behavior and gene expression. We show that the majority of upper jaw shape variation can be explained by progressive changes in the spatial organization and mitotic activity of midfacial growth zones controlled by SHH signaling. In addition, nonlinearity between our treatment doses and phenotypic outcomes suggests that threshold effects in SHH signaling may play a role in variability in midfacial malformations such as holoprosencephaly (HPE). Together, these results provide novel insight into the generation of facial morphology, and demonstrate the value of quantifying variation for our understanding of development and disease.

KEY WORDS: Population variation, Cell signaling, Cranial neural crest cells, Geometric morphometrics, Chick

INTRODUCTION

Sonic hedgehog (SHH) signaling plays an essential role in the epithelial-mesenchymal interactions that control proximodistal extension and dorsoventral polarity of the vertebrate upper jaw (Hu et al., 2003; Marcucio et al., 2005; Hu and Marcucio, 2009). *Shh* is first expressed in the forebrain prior to outgrowth of the facial prominences. As neural crest cells migrate into the midface, *Shh* is activated in the adjacent epithelium, and this frontonasal ectodermal zone (or 'FEZ') acts as a signaling center that controls growth (Marcucio et al., 2005). Blockade of SHH signaling in the forebrain inhibits *Shh* expression in the FEZ, downregulates target genes in the adjacent mesenchyme (e.g. *Ptc1*, *Gli1*), and leads to a narrow and truncated face (Marcucio et al., 2005). Experimental activation of SHH signaling in the forebrain expands *Shh* neuroepithelial expression dorsally, alters the pattern of *Shh* expression in the FEZ, lateralizes proliferative zones in the facial mesenchyme, and causes an abnormally wide upper jaw and face (Hu and Marcucio, 2009).

These experimental outcomes are similar to human disease phenotypes associated with altered SHH signaling. In holoprosencephaly (HPE), SHH signaling is often reduced, and midline malformations range from hypotelorism and facial hypoplasia to complete cyclopia (DeMeyer et al., 1964; Muenke and Beachy, 2000; Muenke and Cohen, 2000). In Greig cephalopolysyndactyly (GCPS) and Gorlin syndrome, mutations enhance SHH-signaling activity (GLI3 and PTC, respectively) and phenotypic outcomes range from hypertelorism to midline clefts (Balk and Biesecker, 2008). Of note, family members of afflicted individuals frequently manifest subclinical midfacial phenotypes (Cohen and Sullik, 1992; Muenke and Cohen, 2000; Balk and Biesecker, 2008), implicating genetic variation in the SHH-signaling pathway as a potential contributor to normal midfacial shape. Together, this evidence suggests that there is a predictive relationship between the magnitude of SHH signaling, and the size, spatial organization and activity of midfacial growth zone(s) that are controlled by the FEZ. In addition, as SHH protein frequently acts as a diffusible morphogen (Ingham and McMahon, 2001; McMahon et al., 2003; Hooper and Scott, 2005), this variation may be generated through concentration-dependent changes in growth.

To test this idea, we performed two dose-response experiments in which we varied activation of the SHH-signaling pathway in the brain of avian embryos by adding exogenous factors to either reduce or increase SHH ligand concentration before facial formation. We next used high-resolution micro-computed tomography (μCT) and microscopy to image treated and control embryos, and landmark-based geometric morphometrics (GM) to quantify and compare facial shape variation (Bookstein, 1996; Zelditch et al., 2004). Specifically, we used Procrustes superimposition to remove the effects of orientation and scale, and principal components analysis (PCA) to identify two- and three-dimensional shape variation that correspond to doses. These differences were visualized as displacements of landmarks, wireframe grids or 3D surfaces (e.g. Young et al., 2007; Boughner et al., 2008; Parsons et al., 2008). Next, in individual embryos we measured the activation of the SHH-signaling pathway in the brain via quantitative RT-PCR, and growth in the midfacial mesenchyme via quantification of cell proliferation. Finally, we assessed the relationship of doses to population-level variation in quantitative gene expression, growth and individual phenotypic outcomes.

[1]University of California, San Francisco, Department of Orthopaedic Surgery, Building 9, Room 342, 2550 23rd Street, San Francisco, CA 94110, USA. [2]University of California, San Francisco, School of Medicine, San Francisco, CA 94143, USA. [3]University of Calgary, Department of Cell Biology and Anatomy, 3330 Hospital Drive NW, Calgary, AB, T2N 4N1, Canada.

*These authors contributed equally to this work
†Author for correspondence (marcucio@orthosurg.ucsf.edu)

Accepted 4 August 2010

MATERIALS AND METHODS

Embryo sample and preparation

Fertilized chicken eggs (*Gallus gallus*, Rhode Island Red) were incubated for 48 hours [Hamburger-Hamilton (HH) stage 10], 1.0 ml of albumin was removed, and the shell was opened to directly access the embryo for experimental treatment (see below). At both 72 hours and 13 days post-treatment, embryos were collected and fixed overnight at 4°C in 4% paraformaldehyde (PFA).

5E1 SHH antibody and SHH-N bead treatment

5E1 anti-SHH antibody cells and 40-1A anti-β-galactosidase antibody control cells were cultured in DMEM high-glucose media with 10% fetal bovine serum, 1% L-glutamine, and penicillin-streptomycin. Media (0.15 μl) containing cells at five concentrations (4×10^7, 2×10^7, 1×10^7, 5×10^6 and 2.5×10^6 cells/ml) (n=102) or control 401-A cells (4×10^7 cells/ml) (n=21) was injected into the anterior neural tube of one set of embryos. A second set of embryos was implanted with beads soaked in either SHH-N protein at three concentrations (0.4, 0.8 and 1.6 mg/ml) (n=36) or with a PBS bead (control) (n=16). Wild-type untreated embryos comprised the remaining sample (n=30). The highest titer in each experiment was determined previously to maximally repress or activate the pathway (Hu et al., 2003; Marcucio et al., 2005; Hu and Marcucio, 2009).

Geometric morphometric shape analysis

For 3D data, embryos were removed from PFA, washed three times for 10 minutes each in PBS and transferred to Bouin's Solution. Fixed embryos were scanned via micro-computed tomography at a resolution of 6.25 μm and 3D surfaces were created in Amira 4.1.2 (Mercury Systems). Sixty-seven landmarks covering the face, mouth, eyes and forebrain were applied to each surface and the raw coordinates (x, y, z) recorded in Landmark (lists are available on request) (Wiley et al., 2005). For 2D data, specimens were placed in PBS, imaged in anterior view (2.0×) and transferred to PFA. The coordinates (x, y) of 45 landmarks were recorded from digital images in ImageJ 1.43s6 (http://rsb.info.nih.gov/ij). For both datasets, raw landmark coordinates were averaged across the axis of symmetry to minimize side-to-side variation (i.e. yaw), and Procrustes superimposition was implemented to remove the effect of alignment, rotation and scale (Zelditch et al., 2004). These transformed shape data were regressed against normal shape-size allometry to remove the effect of size heterogeneity and the residuals were subjected to principal components analysis (PCA) in MorphoJ 1.02b (http://www.flywings.org.uk/MorphoJ_page.htm).

Cell proliferation

A subsample (n=26) was injected with 5-bromo-deoxyuridine (BrdU) 20 minutes prior to collection, and after shape analysis were dehydrated in a graded ethanol series, embedded in paraffin, and sectioned coronally through the frontonasal region anterior to the optic recess. Proliferating cells were detected via immunohistochemisty and 3,3′ diaminobenzidine (DAB). Mitotic activity was estimated as the number of positively stained mesenchymal cells divided by the total number of mesenchymal cells.

Quantitative RT-PCR (qRT-PCR)

In a subsample (n=16) the neuroepithelium was dissected from the face and separated from other tissues with dispase (Sigma-Aldrich), placed in Trizol (Invitrogen), centrifuged to extract and isolate RNA, and cDNA created via reverse transcription. qRT-PCR for chicken *Shh* transcripts was performed with the following primer sets: forward, 5′-CACATCCACTGCTC-CGTCAA-3′; reverse, 5′-GTCGAGGAAGGTGAGGAAGT-3′.

Whole-mount in situ hybridization

Gene expression was analyzed by whole-mount in situ hybridization of embryos using dioxigenin (DIG)-labeled riboprobes synthesized from linearized chicken-specific *Shh* subclones and following standard protocols.

RESULTS AND DISCUSSION

Reduced SHH signaling caused structural narrowing of the frontonasal process, progressive hypotelorism, and medial maxillary rotation, whereas increased SHH signaling caused widening of the midface, frontonasal hypoplasia and bifurcation, and lateral divergence of the maxillaries (Fig. 1A-C). Both loss- and gain-of-function experiments affected not only the shape and size of the midface, but also the shape and size of the eyes, which has been documented previously (Marcucio et al., 2005; Hu and Marcucio, 2009; Yamamoto et al., 2009). In addition, external dorsal head shape was altered in both experiments. PCA of the Procrustes-transformed shape data indicated that changes to the midface explained the largest proportion of variation in PC1 (62.8%), and were independent of variation in eye and brain shape on PC2 (17.2%). Concordant with this finding, when we examined internal 3D brain shape using μCT reconstructions we observed that whereas the dorsal region of the brain changed in size and shape (Fig. 1B), the area adjacent to the face (corresponding to the ventral telencephalon anterior to the optic recess) was not associated with facial changes (Fig. 1C). We also noted that whereas eye shape was altered in both experiments, in both cases they became smaller, suggesting SHH signaling has an independent effect on eye morphology that is particularly sensitive to concentration. When plotted against treatment dose, the PC1 of midfacial landmarks (75.9% shape variation) shows a highly significant correlation within each experiment (5E1: r^2=0.637, P<0.001; SHH-N: r^2=0.569, P<0.001) (Fig. 1A). This relationship appears to scale in a nonlinear fashion, particularly when the pathway is repressed, with small doses initially yielding large differences in phenotypic outcomes but a reduced effect on morphology despite progressively higher doses.

To better understand how this phenotypic variation was generated, we next assessed gene expression in the facial epithelia via in situ hybridization and found that the mediolateral width of the FEZ was proportional to the width of the face and the dose delivered to the brain (Fig. 1D). Previously, we have shown that the FEZ regulates growth via cell proliferation and not cell death in the facial mesenchyme (Marcucio et al., 2005; Hu and Marcucio, 2009), and here we further found a significant correlation between mitotic activity in the midface and shape outcome (r^2=0.722, P<0.001) (Fig. 2A). In addition, we previously have shown that activation of SHH signaling in the brain led to an increase in the size of the *Shh* expression domain in the telencephalon, changes in the spatial organization of the FEZ and alteration of the location of growth zones in the facial mesenchyme (Hu and Marcucio, 2009). Here, qRT-PCR results demonstrate that increased *Shh* expression in the brain is significantly correlated with shape (log-linear, r^2=0.844, P<0.001) (Fig. 2B). Combined with previous data on cell proliferation from activation experiments (Hu and Marcucio, 2009), the changes in *Shh* expression from in situ hybridization suggest that decreased signaling in the brain affects the size of the FEZ and the growth potential of the facial mesenchyme, whereas increasing SHH-signaling above normal levels primarily affects the spatial organization of the FEZ, perhaps by inhibiting midline expression (Fig. 1E). Both sets of data are consistent with the direction of midfacial growth described by the embryonic shape analysis as activation of the SHH pathway in the brain generated a wider midface that corresponds to the bilateralization of *Shh* expression in the FEZ and the lateralization of the growth zones in the mesenchyme. This conclusion is further supported by phenotypic outcomes at 13 days post treatment, where decreased SHH-signaling activity led to a progressive narrowing and shortening of the midfacial skeleton, whereas increased activity yielded progressively wider midfaces with median clefts (Fig. 1F).

Together, these results provide quantitative support for the hypothesis that variation in SHH-signaling from the forebrain contributes to continuous phenotypic variation in upper jaw shape,

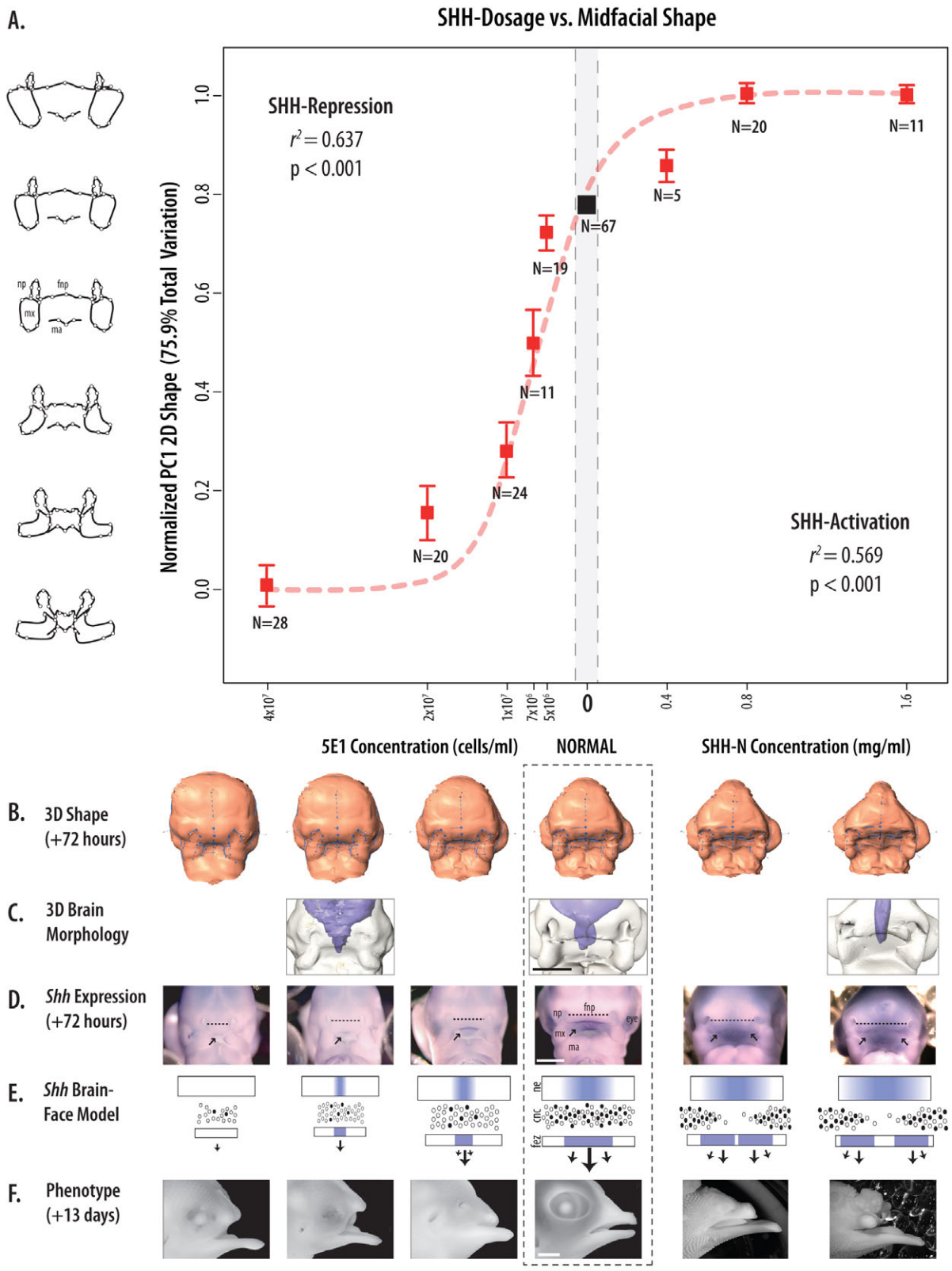

Fig. 1. Experimental results. (**A**) Relationship of dosage to mean midfacial shape scores from both experiments (5E1: r^2=0.637, P<0.001; SHH-N: r^2=0.569, P<0.001; bars represent s.e.). y-axis represents the mathematical deformation of the mean midfacial landmark configuration. Broken line shows maximum likelihood fit of a nonlinear Hill equation (Hill coefficient n=8.73). (**B**) Relative 3D-shape changes using a thin-plate spline transformation of surface landmark data scaled to a common size. (**C**) Internal brain shape (purple). (**D**) *Shh* whole-mount in situ hybridization (arrows, positive signal). (**E**) Schematic transverse section illustrating the proposed relationship between *Shh* expression (blue) in the brain (neuroectoderm, ne), face (frontoectodermal zone, fez) and cell proliferation (white, non-proliferating; black, proliferating). Arrows show direction of midfacial growth. Frontonasal process, fnp; nasal pits, np; maxillary prominences, mx. (**F**) External facial shape 13 days post treatment. Scale bars: 1 mm in C,D; 2 mm in F.

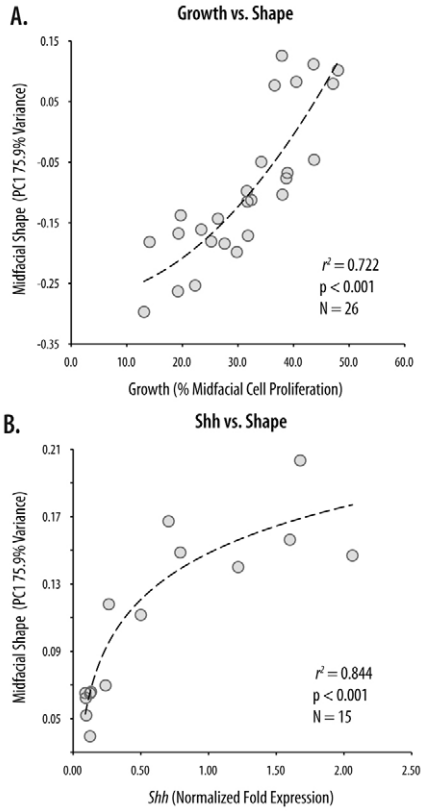

Fig. 2. Midfacial shape, growth and gene expression. (**A**) Percentage of mitotically active cells in the repression experiment (r^2=0.722, n=26, P<0.001). (**B**) *Shh* expression levels in the brain in the activation experiment (r^2=0.844, n=16, P<0.001).

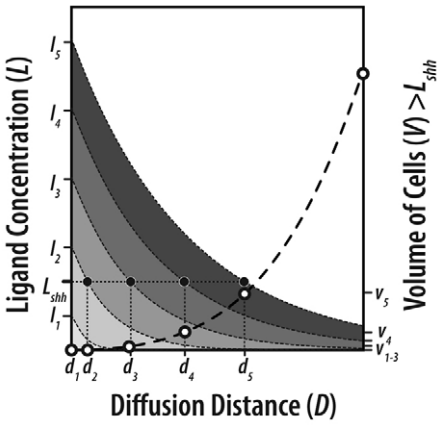

Fig. 3. Hypothetical model of SHH signaling and growth. SHH concentration gradient in the midface modeled as $L(x)=L\cdot exp(-x/C)$ where L is the ligand concentration and C is the decay coefficient (Eldar et al., 2003). Downstream targets of the pathway, such as those promoting cell cycle acceleration, are hypothesized to be rapidly activated at L_{shh} (e.g. Lai et al., 2004), and $D_n(L)$ is the linear distance from the ligand signaling source where $L_n>L_{shh}$. The volume of cells (V_n) where $L_n>L_{shh}$ for any D_n is approximately equal to $4/6\cdot\pi\cdot D_n^3$ (i.e. half the volume of a sphere with radius D_n). This model predicts that mutations affect growth by altering either (1) ligand concentration (L) or decay (C), or (2) the sensitivity of cells to ligand concentration (i.e. L_{shh}), and linear changes in concentration result in nonuniform responses. Not shown in this figure is that the FEZ may be inhibited in the midline above a crucial concentration of SHH in the brain, thereby limiting the maximal effective FEZ size and lateralizing growth zones.

and demonstrates that morphological differences are caused by the effect of signaling variation on the size, spatial organization and the mitotic activity of growth zones in the midface. We propose that the effect of SHH-signaling pathway mutations on phenotypic outcome is ultimately driven by their effect on concentration-related parameters. In other words, mutations contribute to variation either via their effect on SHH concentration or via the sensitivity of a responding cell to this concentration. In the former, concentration may be affected by mutations to ligand synthesis, activation (e.g. *Shh*), accumulation (e.g. *Disp1*) (Tian et al., 2004; 2005; Etheridge et al., 2010) or transport (e.g. *Cdo*, *Boc*, *Gas1*) (Saha and Schaffer, 2006; Tenzen et al., 2006; Zhang et al., 2006; Allen et al., 2007; Seppala et al., 2007). In the latter, the concentration at which a responding cell reacts may be affected by variation in its receptor affinity to SHH (e.g. via *Ptc*) (Ingham and McMahon, 2001), ability to transduce SHH signals (e.g. via *Smo*) (Taipale et al., 2002), or to sense SHH (e.g. in primary ciliopathies) (Tobin et al., 2008). In both cases, the ultimate phenotypic effect would be predicted to be similar as they ultimately impact the proportion of cells where growth is actively promoted by SHH. Supporting this idea, allelic variation in SHH-pathway genes is known to yield a range of phenotypic effects in mice that qualitatively parallel those described here, and the relative effect appears to be proportional to the function of the gene within the pathway. Thus, although knockout of *Cdo* has a small phenotypic effect concordant with its function as a co-receptor that affects local SHH concentration, *Shh* heterozygosity exacerbates this effect by reducing the ligand production at the signaling source (Tenzen et al., 2006). In individuals with SHH-associated diseases such as HPE, poor genotype-phenotype correlations may therefore result from the combination of multiple genes of small additive or epistatic effect contributing to overall severity (Hardy and Singleton, 2009; Manolio et al., 2009). This idea is similar to hypotheses postulating either that additional genetic or environmental perturbations lead to more severe phenotypes (i.e. 'second hit') (Ming and Muenke, 2002), or that modifier genes modulate SHH signaling within individuals (Dipple and McCabe, 2000).

The dose-response relationship we observe here is further suggestive of a threshold effect where small changes in protein concentration initially cause large effects on mean phenotypic responses but these become progressively attenuated despite progressively higher doses. Support for this idea requires a more direct measure of SHH signal strength or ligand concentration than dose alone, but additional evidence suggests how such nonlinearity might be generated via concentration effects. Specifically, SHH frequently acts as a morphogen gradient (Hooper and Scott, 2005), and alternative cellular behaviors such as patterning and growth are thought to be generated via the activation of downstream targets at specific SHH concentrations (Lai et al., 2004; Ulloa and Briscoe, 2007), which appears to be a general feature of the pathway (Lai et al., 2004). We speculate that SHH activity in the forebrain establishes the size and location of the FEZ, whereas FEZ size generates a SHH gradient in the mesenchyme (e.g. Fig. 1E). A FEZ induced SHH gradient would then generate differential growth by accelerating the cell cycle above basal rates via upregulation of targets such as *Cyclin D2* and *N-myc*. Ligand concentration determines a volume of proliferating cells, and this would be

proportional to the cube of the effective diffusion distance (Fig. 3). Activation of SHH in the brain above normal physiological levels may not further accelerate this process because at sufficiently high concentrations SHH in the forebrain appears to shut off FEZ activity in the midline, splitting expression into two lateral proliferative domains (Fig. 1D) (Hu and Marcucio, 2009). In this model, linear changes to ligand concentration would cause nonlinear responses in the number of responsive cells, and on the proportion of proliferating cells, growth rate and shape. These predictions are amenable to future experimental validation, and suggest that variable SHH-related midfacial phenotypes result from the proximity of normal signaling levels to crucial threshold concentrations above which growth zones are stimulated. If confirmed, such nonlinearity could help explain increased variability in diseases associated with reduced SHH signaling such as HPE, as some genotypes exhibit higher variability than others.

In summary, this analysis shows how a quantitative approach to development can help not only to validate previously qualitative hypotheses but also to generate novel and testable alternatives (see also Cooper and Albertson, 2008; Oates et al., 2009). Although these results specifically address the relationship of SHH-signaling strength to midfacial growth and shape, this approach can be applied to other related cell-signaling pathways (e.g. BMP, WNT, FGF, etc.) and anatomical structures (e.g. the autopod). Future research that explicitly incorporates a quantitative approach into experimental design will help to place developmental biology in a population-level framework and further our understanding of organismal morphogenesis and variation.

Acknowledgements

We thank W. Liu, X. Li, Y. Xu, F. Smith, S. Keena, R. A. Schneider and O. Klein for comments and assistance. This research was supported by National Institutes of Health (NIH) grant F32DE018596 (N.M.Y.), by a Howard Hughes Medical Institute Medical Research Training Fellowship (H.J.C.), and by NIH/NIDCR R01DE018234 (R.S.M.) and R01DE019638 (R.S.M., B.H., N.M.Y.). Deposited in PMC for release after 12 months.

Competing interests statement

The authors declare no competing financial interests.

Author contributions

N.M.Y., B.H. and R.S.M. designed the research and experiments. N.M.Y., H.J.C. and D.H. performed the experiments and collected the data. N.M.Y., B.H. and R.S.M. analyzed the data. All authors contributed to the writing of the paper.

References

Allen, B. L., Tenzen, T. and McMahon, A. P. (2007). The Hedgehog-binding proteins Gas1 and Cdo cooperate to positively regulate Shh signaling during mouse development. *Genes Dev.* **21**, 1244-1257.

Balk, K. and Biesecker, L. G. (2008). The clinical atlas of Greig cephalopolysyndactyly syndrome. *Am. J. Med. Genet.* **146A**, 548-557.

Bookstein, F. L. (1996). *Morphometric Tools for Landmark Data: Geometry and Biology.* Cambridge: Cambridge University Press.

Boughner, J. C., Wat, S., Diewert, V. M., Young, N. M., Browder, L. W. and Hallgrímsson, B. (2008). Short-faced mice and the developmental interactions between the brain and the face. *J. Anat.* **213**, 646-662.

Cohen, M. M. and Sulik, K. K. (1992). Perspectives on holoprosencephaly, Part II: Central nervous system, craniofacial anatomy, syndrome commentary, diagnostic approach, and experimental studies. *J. Craniofac. Genet. Dev. Biol.* **12**, 196-224.

Cooper, W. J. and Albertson, R. C. (2008). Quantification and variation in experimental studies of morphogenesis. *Dev. Biol.* **321**, 295-302.

Cordero, D., Marcucio, R., Hu, D., Gaffield, W., Tapadia, M. and Helms, J. A. (2004). Temporal perturbations in sonic hedgehog signaling elicit the spectrum of holoprosencephaly phenotypes. *J. Clin. Invest.* **114**, 485-494.

DeMeyer, W. E., Zeman, W. and Palmer, C. G. (1964). The face predicts the brain: diagnostic significance of median facial anomalies for holoprosencephaly (arhinencephaly). *Pediatrics* **34**, 256-263.

Dipple, K. M. and McCabe, E. R. (2000). Phenotypes of patients with 'simple' Mendelian disorders are complex traits: thresholds, modifiers, and systems dynamics. *Am. J. Hum. Genet.* **66**, 1729-1735.

Eldar, A., Rosin, D., Shilo, B. Z. and Naama, B. (2003). Self-enhanced ligand degradation underlies robustness of morphogen gradients. *Dev. Cell* **5**, 635-646.

Etheridge, L. A., Crawford, T. Q., Zhang, S. and Roelink, H. (2010). Evidence for a role of vertebrate Disp1 in long-range Shh signaling. *Development* **137**, 133-140.

Hardy, J. and Singleton, A. (2009). Genomewide association studies and human disease. *New Engl. J. Med.* **360**, 1759-1768.

Hooper, J. E. and Scott, M. P. (2005). Communicating with Hedgehogs. *Nat. Rev. Mol. Cell. Biol.* **6**, 306-317.

Hu, D. and Marcucio, R. S. (2009). A SHH-responsive signaling center in the forebrain regulates craniofacial morphogenesis via the facial ectoderm. *Development* **136**, 107-116.

Hu, D., Marcucio, R. S. and Helms, J. A. (2003). A zone of frontonasal ectoderm regulates patterning and growth in the face. *Development* **130**, 1749-1758.

Ingham, P. W. and McMahon, A. P. (2001). Hedgehog signaling in animal development: paradigms and principles. *Genes Dev.* **15**, 3059-3087.

Lai, K., Robertson, M. J. and Schaffer, D. V. (2004). The sonic hedgehog signaling system as a bistable genetic switch. *Biophys. J.* **86**, 2748-2757.

Manolio, T. A., Brooks, L. D. and Collins, F. S. (2009). A HapMap harvest of insights into the genetics of common disease. *J. Clin. Invest.* **118**, 1590-1605.

Marcucio, R. S., Cordero, D. and Helms, J. A. (2005). Molecular interactions coordinating the development of the forebrain and face. *Dev. Biol.* **284**, 48-61.

McMahon, A. P., Ingham, P. W. and Tabin, C. J. (2003). Developmental roles and clinical significance of hedgehog signaling. *Curr. Top. Dev. Biol.* **53**, 1-114.

Ming, J. E. and Muenke, M. (2002). Multiple hits during early embryonic development: digenic diseases and holoprosencephaly. *Am. J. Hum. Genet.* **71**, 1017-1032.

Muenke, M. and Beachy, P. A. (2000). Genetics of ventral forebrain development and holoprosencephaly. *Curr. Opin. Genet. Dev.* **10**, 262-269.

Muenke, M. and Cohen, M. M. (2000). Genetic approaches to understanding brain development: holoprosencephaly as a model. *Ment. Retard. Dev. Disab. Res. Rev.* **6**, 15-21.

Oates, A. C., Gorfinkiel, N., Gozález-Gaitán, M. and Heisenberg, C. P. (2009). Quantitative approaches in developmental biology. *Nat. Rev. Genet.* **10**, 517-530.

Parsons, T. E., Kristensen, E., Hornung, L., Diewert, V. M., Boyd, S. K., German, R. Z. and Hallgrímsson, B. (2008). Phenotypic variability and craniofacial dysmorphology: increased shape variance in a mouse model for cleft lip. *J. Anat.* **212**, 135-143.

Saha, K. and Schaffer, D. V. (2006). Signal dynamics in Sonic hedgehog tissue patterning. *Development* **133**, 1411-1411.

Seppala, M., Depew, M. J., Martinelli, D. C., Fan, C. M., Sharpe, P. T. and Cobourne, M. T. (2007). *Gas1* is a modifier for holoprosencephaly and genetically interacts with sonic hedgehog. *J. Clin. Invest.* **117**, 1575-1584.

Taipale, J., Cooper, M. K., Maiti, T. and Beachy, P. A. (2002). Patched acts catalytically to suppress the activity of Smoothened. *Nature* **418**, 892-897.

Tenzen, T., Allen, B. L., Cole, F., Kang, J. S., Krauss, R. S. and McMahon, A. P. (2006). The cell surface membrane proteins Cdo and Boc are components and targets of the Hedgehog signaling pathway and feedback network in mice. *Dev. Cell* **10**, 647-656.

Tian, H., Tenzen, T. and McMahon, A. P. (2004). Dose dependency of *Disp1* and other hedgehog signaling components in the mouse. *Development* **131**, 4021-4033.

Tian, H., Jeong, J., Harfe, B. D., Tabin, C. J. and McMahon, A. P. (2005). Mouse Disp1 is required in sonic hedgehog-expressing cells for paracrine activity of the cholesterol-modified ligand. *Development* **132**, 133-142.

Tobin, J. L., Di Franco, M., Eichers, E., May-Simera, H., Garcia, M., Yan, J., Qunlan, R., Justice, M. J., Hennekam, R. C., Briscoe, J. et al. (2008). Inhibition of neural crest migration underlies craniofacial dysmorphology and Hirschprung's disease in Bardet-Biedl syndrome. *Proc. Natl. Acad. Sci. USA* **105**, 6714-6719.

Ulloa, F. and Briscoe, J. (2007). Morphogens and the control of cell proliferation and patterning in the spinal cord. *Cell Cycle* **6**, 2640-2649.

Wiley, D. F., Amenta, N., Alacantara, D. A., Ghosh, D., Kil, Y. J., Delson, E., Harcourt-Smith, W., Rohlf, F. J., St. John, K. and Hamann, B. (2005). Evolutionary Morphing. In *Proceedings of IEEE Visualization 2005*. Minneapolis, MN: IDAV.

Yamamoto, Y., Byerly, M. S., Jackman, W. R. and Jeffery, W. R. (2009). Pleiotropic functions of embryonic *sonic hedgehog* expression link jaw and taste bud amplification with eye loss during cavefish evolution. *Dev. Biol.* **330**, 200-211.

Young, N. M., Wat, S., Diewert, V. M., Browder, L. W. and Hallgrímsson, B. (2007). Comparative morphometrics of embryonic facial morphogenesis: implications for cleft-lip etiology. *Anat. Rec.* **290**, 123-139.

Zelditch, M. L., Swiderski, D. L., Sheets, H. D. and Fink, W. L. (2004). *Geometric Morphometrics for Biologists: a Primer*. New York: Academic Press.

Zhang, W., Kang, J. S., Cole, F., Yi, M. J. and Krauss, R. S. (2006). Cdo functions at multiple points in the Sonic Hedgehog pathway, and Cdo-deficient mice accurately model human holoprosencephaly. *Dev. Cell* **10**, 657-665.